

Kinematic Modeling of Chained Form Mobile Robot

Jae Yong Han, Jae Hoon Lee, Byung-Ju Yi, and Whee Kuk Kim*

School of Electrical Engineering and Computer Science, HANYANG University,
1271, Sa 1-dong, Sangrok-ku, Ansan, Kyungki-do, Korea
(Tel : +82-31-400-5218; E-mail : bj@hanyang.ac.kr)

*Department of Control and Instrumentation Engineering, KOREA University

Abstract: Chained form mobile robots have been studied from the viewpoint of the control and analysis of nonholonomic mechanical systems in literature. However, researches for the detailed closed form kinematic modeling are rarely progressed. Nothing that a chained form mobile robot can be considered as a parallel system including several chains and wheels, the transfer method using augmented generalized coordinates is applied to obtain inverse and forward kinematic models of chained form mobile robots. Various numerical simulations are conducted to verify the effectiveness of the suggested kinematic model.

Keywords: chained form mobile robot, kinematic model.

1. INTRODUCTION

Laumond[2] showed the controllability of a multiple trailer system. Murray and Sastry[3] provided the way of developing many controllers to steer and to stabilize nonholonomic mechanical system, including the multiple trailer system. And Chung[4] found most controllable passive trailer system by comparing tracking error and stability of various passive trailers that have different features according to their mechanical structure and parameters.[4]

Until now, chained mobile robot systems have been studied mostly from the viewpoint of the control and analysis of nonholonomic mechanical systems. On the other hand, the closed form kinematic modeling has not been mentioned in literature, which would be beneficial in the analysis and design of such systems.

This paper focuses on a closed-form kinematic modeling for a chained mobile robot system, which will in turn be very useful in kinematic analysis, design and modeling of systems with similar structures. In section 2, the kinematic model of a 3 wheeled 2 DOF mobile robot is described. Then in section 3, the kinematic model of the chained form mobile robot is presented. Section 4 illustrates simulation results for the chained form mobile robot. Finally, some concluding remarks and future works are presented in section 5.

2. KINEMATIC MODEL OF 3 WHEELS AND 2 DOF MOBILE ROBOT

In this section, the kinematic model of a mobile robot with two fixed wheels and a caster wheel is described[1].

2.1 Kinematic model of a fixed wheel

Fig. 1 represents a schematic of a mobile robot having two fixed wheels and a caster wheel. The platform of the mobile robot is a triangle with width l and length $(a+b)$. The radius of each wheel is r , and the length of the link of the caster wheel is d . The local coordinate body frame is attached at the center of the platform of the mobile robot.

The output velocity vector of the mobile robot and the joint velocity vector of the two fixed wheels are defined as

$$\dot{u} = (v_{bx} \quad v_{by} \quad \omega)^T, \tag{1}$$

$${}_i\dot{\phi}^* = (\dot{\eta}_i, \dot{\theta}_i, v_{ski})^T, \quad (i=1,2) \tag{2}$$

respectively, where $\dot{\eta}_i$ and v_{ski} represent a rotational velocity about the \hat{Z} axis and a skidding velocity along the the direction of the wheel axis. Here, v_{ski} is included as an augmented velocity variable. The velocity relationship between the output vector of the mobile robot and the joint variables of each of the two wheels can be written in a matrix form as

$$\dot{u} = [{}_iG_{\phi^*}^u] {}_i\dot{\phi}^*, \quad (i=1,2) \tag{3}$$

where

$$[{}_iG_{\phi^*}^u] = \begin{bmatrix} y_i & 0 & 1 \\ -x_i & r & 0 \\ 1 & 0 & 0 \end{bmatrix}. \tag{4}$$

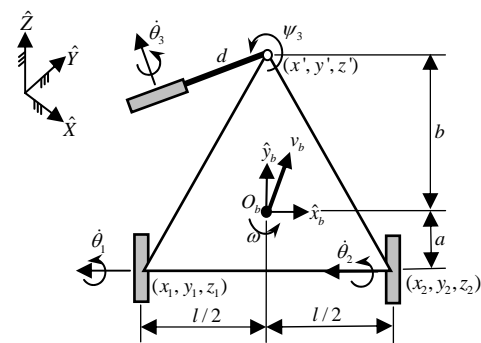


Fig.1. 2 DOF mobile robot

When $r \neq 0$, the inverse kinematics of Eq. (3) is obtained as

$${}_i\dot{\phi}^* = -\frac{1}{r} \begin{bmatrix} 0 & 0 & -r \\ 0 & -1 & -x_i \\ -r & 0 & ry_i \end{bmatrix} \dot{u}. \tag{5}$$

2.2 Kinematic model of a caster wheel

The kinematics of a caster wheel is derived as [1]

$$\dot{u} = [{}_3G_\phi^u]_3 \dot{\phi}, \tag{6}$$

where

$$[{}_3G_\phi^u] = \begin{bmatrix} -d \cos \psi_3 + y' & r \sin \psi_3 & y' \\ d \sin \psi_3 - x' & r \cos \psi_3 & -x' \\ 1 & 0 & 1 \end{bmatrix}. \tag{7}$$

The inverse kinematics of Eq. (7) is obtained as

$${}_3\dot{\phi} = [{}_3G_\phi^u] \dot{u}, \tag{8}$$

where

$$[{}_3G_\phi^u] = \frac{1}{dr} \begin{bmatrix} -r \cos \psi_3 & r \sin \psi_3 & rx' \sin \psi_3 + ry' \cos \psi_3 \\ d \sin \psi_3 & d \cos \psi_3 & dx' \cos \psi_3 - dy' \sin \psi_3 \\ r \cos \psi_3 & -r \sin \psi_3 & dr - rx' \sin \psi_3 - ry' \cos \psi_3 \end{bmatrix}. \tag{9}$$

2.3 Kinematic model of a single mobile robot

The kinematic model of a single mobile robot driven by two fixed wheels(i.e., differential driven) is derived in this section[1]. The inverse Jacobian matrix for each fixed wheel is obtained by including the skidding velocity vector as a augmented variable($v_f = v_{sk1} = v_{sk2}$) into the input vector. The inverse kinematic relationship between an augmented joint velocity vector($\dot{\phi}_a = (\dot{\theta}_1 \ \dot{\theta}_2 \ v_f)^T$) and the output velocity vector($\dot{u} = (v_{bx} \ v_{by} \ \omega)^T$) is obtained as

$$\dot{\phi}_a = -\frac{1}{r} \begin{bmatrix} 0 & -1 & \frac{l}{2} \\ 0 & -1 & -\frac{l}{2} \\ -r & 0 & -ar \end{bmatrix} \dot{u} \tag{10}$$

by selecting three rows corresponding to the three input variables from Eq. (5).

The forward kinematic relationship between the augmented input vector and the output velocity vector of a single mobile robot is obtained as

$$\dot{u} = \frac{r}{l} \begin{bmatrix} a & -a & \frac{l}{r} \\ \frac{l}{2} & \frac{l}{2} & 0 \\ -1 & 1 & 0 \end{bmatrix} \begin{bmatrix} \dot{\theta}_1 \\ \dot{\theta}_2 \\ v_f \end{bmatrix} \tag{11}$$

by taking inverse of Eq. (10).

If there is no skidding velocity, the forward kinematic equation is obtained as

$$\dot{u} = \frac{r}{l} \begin{bmatrix} a & -a \\ \frac{l}{2} & \frac{l}{2} \\ -1 & 1 \end{bmatrix} \begin{bmatrix} \dot{\theta}_1 \\ \dot{\theta}_2 \end{bmatrix} \tag{12}$$

by substituting constraint $v_f = 0$ into Eq. (11).

3. KINEMATIC MODELING OF CHAINED FORM MOBILE ROBOT

3.1 Kinematic modeling

The closed-form kinematic model of a chained form mobile robot consisting of n trailers is derived in this section. Fig. 2 represents the kinematic diagram of a chained form mobile robot. It is assumed for simplicity that each mobile robot is a differential driven type and two adjacent mobile robots are connected by a revolute joint. Chung, et al[4] suggested that this type of module exhibits the best kinematic performance as compared to other previous types. To obtain the kinematic relationship among trailers, every trailer following its front trailer is modeled as a caster wheel as displayed in Fig. 3. More specifically, the following trailer can be visualized as two caster wheels having two offsets, as shown in Fig. 4.

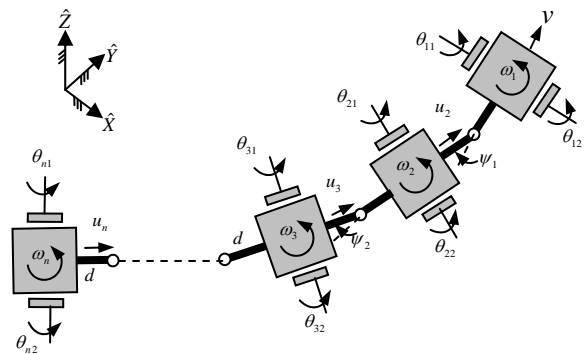


Fig. 2. Chained form mobile robot

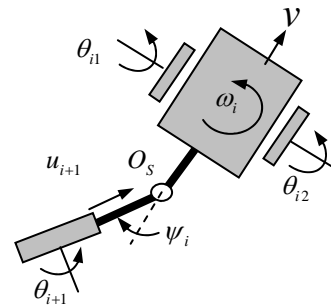


Fig. 3. Modeling the following trailer as a caster wheel

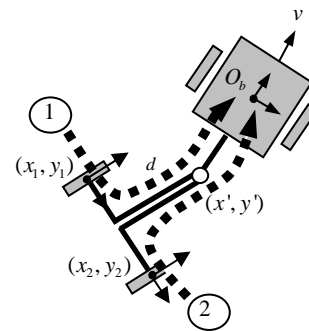


Fig. 4. Path of velocity constraints

To obtain the kinematic model of the system, we apply the above mentioned kinematic modeling method of the caster

wheel which was described in the previous section.

The kinematic model relating the output vector of the first trailer to the joint vector in the first path of Fig.4 is obtained as

$$\dot{u}_i = [{}_{i1}G_\phi^u] \dot{\phi}_{i1}, \quad (13)$$

where

$$[{}_{i1}G_\phi^u] = \begin{bmatrix} y_1 \cos \psi_i - x_1 \sin \psi_i - d \cos \psi_i + y' & r \sin \psi_i & y' \\ -y_1 \sin \psi_i - x_1 \cos \psi_i + d \sin \psi_i - x' & r \cos \psi_i & -x' \\ 1 & 0 & 1 \end{bmatrix}, \quad (14)$$

$$\dot{u}_i = (v_{bxi} \ v_{byi} \ \omega_i)^T, \quad (i=1 \sim n-1), \quad (15)$$

$$\dot{\phi}_{i1} = (\dot{\eta}_i, \ \dot{\theta}_{i1}, \ \psi_i)^T, \quad (i=1 \sim n-1). \quad (16)$$

In the same manner, the kinematic model of the second path is obtained as

$$\dot{u}_i = [{}_{i2}G_\phi^u] \dot{\phi}_{i2}, \quad (17)$$

where

$$[{}_{i2}G_\phi^u] = \begin{bmatrix} y_2 \cos \psi_i - x_2 \sin \psi_i - d \cos \psi_i + y' & r \sin \psi_i & y' \\ -y_2 \sin \psi_i - x_2 \cos \psi_i + d \sin \psi_i - x' & r \cos \psi_i & -x' \\ 1 & 0 & 1 \end{bmatrix}, \quad (18)$$

$$\dot{u}_i = (v_{bxi} \ v_{byi} \ \omega_i)^T, \quad (i=1 \sim n-1), \quad (19)$$

$$\dot{\phi}_{i2} = (\dot{\eta}_i, \ \dot{\theta}_{i2}, \ \psi_i)^T, \quad (i=1 \sim n-1). \quad (20)$$

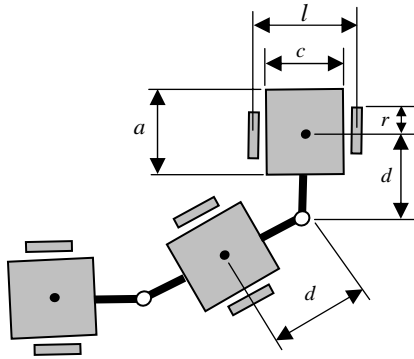


Fig. 5. Layout of trailer

For simplicity, we analyze a three-trailer model displayed in Fig. 5. From Eq. (13), (14), (17), and (18), the inverse kinematics of the second trailer are derived as follows

$$\dot{\phi}_{i1} = [{}_{i1}G_\phi^u]^{-1} \dot{u}_i, \quad (21)$$

where

$$[{}_{i1}G_\phi^u]^{-1} = \frac{1}{dr} \times \begin{bmatrix} -r \cos \psi_i & r \sin \psi_i & -d \cos \psi_i \\ \frac{l}{2} \cos \psi_i + d \sin \psi_i & -\frac{l}{2} \sin \psi_i + d \cos \psi_i & -\frac{l}{2} d \cos \psi_i - d^2 \sin \psi_i \\ r \cos \psi_i & -r \sin \psi_i & dr(1 + \cos \psi_i) \end{bmatrix} \quad (22)$$

and

$$\dot{\phi}_{i2} = [{}_{i2}G_\phi^u]^{-1} \dot{u}_i, \quad (23)$$

where

$$[{}_{i1}G_\phi^u]^{-1} = \frac{1}{dr} \times \begin{bmatrix} -r \cos \psi_i & r \sin \psi_i & -d \cos \psi_i \\ -\frac{l}{2} \cos \psi_i + d \sin \psi_i & \frac{l}{2} \sin \psi_i + d \cos \psi_i & \frac{l}{2} d \cos \psi_i - d^2 \sin \psi_i \\ r \cos \psi_i & -r \sin \psi_i & dr(1 + \cos \psi_i) \end{bmatrix} \quad (24)$$

Now the kinematics of the following trailer can be derived by selecting two rows corresponding to the input joints ($\dot{\theta}_{i+1} = (\dot{\theta}_{(i+1)1}, \ \dot{\theta}_{(i+1)2})^T$) from Eq. (21) and (23):

$$\dot{\theta}_{i+1} = [{}_{ci}G_\phi^u]^{-1} \dot{u}_i = J_{ci}^{-1} \dot{u}_i, \quad (25)$$

where

$$J_{ci}^{-1} = \frac{1}{dr} \times \begin{bmatrix} \frac{l}{2} \cos \psi_i + d \sin \psi_i & -\frac{l}{2} \sin \psi_i + d \cos \psi_i & -\frac{l}{2} d \cos \psi_i - d^2 \sin \psi_i \\ -\frac{l}{2} \cos \psi_i + d \sin \psi_i & \frac{l}{2} \sin \psi_i + d \cos \psi_i & \frac{l}{2} d \cos \psi_i - d^2 \sin \psi_i \end{bmatrix} \quad (26)$$

A chained form mobile robot consists of many trailers connected in series. So the velocities of the wheels of each trailer can be represented as an iterative form given by

$$\dot{\theta}_2 = J_{c1}^{-1} \dot{u}_1, \quad (27)$$

$$\dot{\theta}_3 = J_{c2}^{-1} \dot{u}_2, \quad (28)$$

$$\dot{\theta}_4 = J_{c3}^{-1} \dot{u}_3, \quad (29)$$

$$\vdots$$

$$\dot{\theta}_n = J_{c(n-1)}^{-1} \dot{u}_{n-1}, \quad (30)$$

and

$$\dot{u}_1 = J_1 \dot{\theta}_1, \quad (31)$$

$$\dot{u}_2 = J_2 \dot{\theta}_2, \quad (32)$$

$$\dot{u}_3 = J_3 \dot{\theta}_3, \quad (33)$$

$$\vdots$$

$$\dot{u}_{n-1} = J_{n-1} \dot{\theta}_{n-1}. \quad (34)$$

From the equations (27) through (34), we can obtain the velocity relationship between the leading trailer and the following trailers as

$$\dot{\theta}_2 = [{}^1_2 R J_{c1}^{-1} J_1] \dot{\theta}_1 = P_1 \dot{\theta}_1, \quad (35)$$

$$\dot{\theta}_3 = [{}^1_2 R {}^2_3 R J_{c2}^{-1} J_2 P_1] \dot{\theta}_1 = P_2 \dot{\theta}_1, \quad (36)$$

$$\dot{\theta}_4 = [{}^1_2 R {}^2_3 R {}^3_4 R J_{c3}^{-1} J_3 P_2] \dot{\theta}_1 = P_3 \dot{\theta}_1, \quad (37)$$

$$\vdots$$

$$\dot{\theta}_n = [{}^1_2 R {}^2_3 R \dots {}^{n-1}_n R J_{c(n-1)}^{-1} J_{n-1} P_{n-2}] \dot{\theta}_1 = P_{n-1} \dot{\theta}_1, \quad (38)$$

where

$${}^{i+1}_i R = \begin{bmatrix} \cos \psi_i & -\sin \psi_i & 0 \\ \sin \psi_i & \cos \psi_i & 0 \\ 0 & 0 & 1 \end{bmatrix} \quad (i=1 \sim n-1) \quad (39)$$

By combining the above equations into a matrix form, the final closed-form kinematic model of chained form mobile robots can be found as

$$\dot{\theta}_p = \begin{bmatrix} \dot{\theta}_2 \\ \dot{\theta}_3 \\ \dot{\theta}_4 \\ \vdots \\ \dot{\theta}_n \end{bmatrix} = \begin{bmatrix} P_1 \\ P_2 \\ P_3 \\ \vdots \\ P_{n-1} \end{bmatrix} \dot{\theta}_1. \quad (40)$$

Now, it can be said from Eq. (40) that the motion of the following trailers and kinematically dependent to the front trailer. Though this fact is not new, the closed form given by Eq. (40) is no priori.

3.2 Kinematic relationship between $\dot{\psi}_i$ and \dot{u}_1

From Eq. (21), we can derive the relationship between $\dot{\psi}_i$ and \dot{u}_1 as follows

$$\dot{\psi}_1 = [{}^1G_\phi]_3^u \dot{u}_1 = A_1 \dot{u}_1, \quad (41)$$

$$\dot{\psi}_2 = [{}^2R[{}^2G_\phi]^{-1}]_3 \dot{u}_1 = A_2 \dot{u}_1, \quad (42)$$

$$\dot{\psi}_3 = [{}^2R_3^2 R [{}^3G_\phi]^{-1}]_3 \dot{u}_1 = A_3 \dot{u}_1, \quad (43)$$

\vdots

$$\dot{\psi}_{n-1} = [{}^2R_3^2 R \cdots [{}^{n-2}R [{}^{n-1}G_\phi]^{-1}]_3] \dot{u}_1 = A_{n-1} \dot{u}_1, \quad (44)$$

where $[G]_3$ implies the third row of $[G]$ and

$${}^iR = \begin{bmatrix} \cos \psi_i & -\sin \psi_i & 0 \\ \sin \psi_i & \cos \psi_i & 0 \\ 0 & 0 & 1 \end{bmatrix} \quad (i = 1 \sim n - 1) \quad (45)$$

Writing the above equations into a matrix form yields

$$\dot{\psi}_i = \begin{bmatrix} \dot{\psi}_1 \\ \dot{\psi}_2 \\ \dot{\psi}_3 \\ \vdots \\ \dot{\psi}_{n-1} \end{bmatrix} = \begin{bmatrix} A_1 \\ A_2 \\ A_3 \\ \vdots \\ A_{n-1} \end{bmatrix} \dot{u}_1. \quad (46)$$

From Eq. (46) the steering angles of adjacent mobile robots can be obtained. Thus, Eq (46) is useful in the trajectory planning or in the design of such trailer system.

4. SIMULATION RESULTS

4.1 Description of kinematic parameters

In this paper, we analyze a chained form mobile robot consisting of three trailers as an illustrative example. The kinematic parameters of this system are given in Table 1. Several simulations for following several specified trajectories such as line, curve, and circle are being conducted.

Table 1. Physical dimensions(m) of a trailer

	Length
a	0.09 m
c	0.08 m
d	0.08 m
l	0.1 m
r	0.02 m

4.2 Simulation for a straight line trajectory

The first trajectory is a line with its length of 3m. The mobile robot is commanded to follow this trajectory in 3 seconds. For simplicity, the three trailers are initially aligned on a straight line. Fig. 6 represents the simulation result following the specified line trajectory. It is observed that the mobile robot moves successfully along the vertical line. Note, in particular, that because the chained mobile robot moves along the straight line without steering, the velocity and position trajectories of the wheels of each trailer are the same as shown Fig. 7.

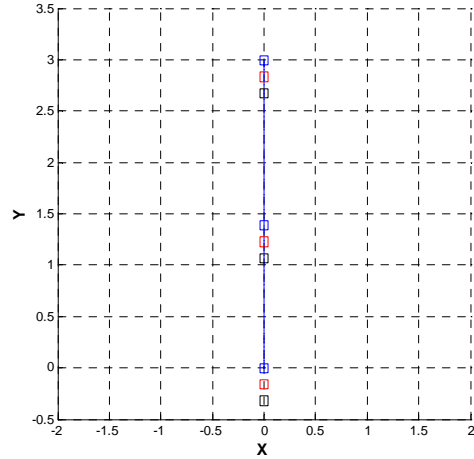
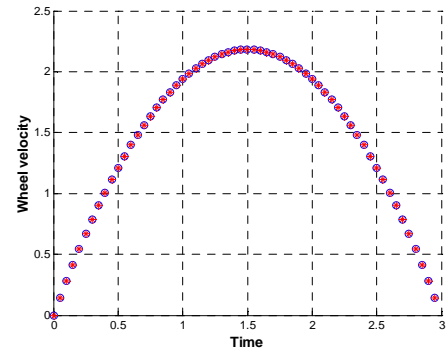
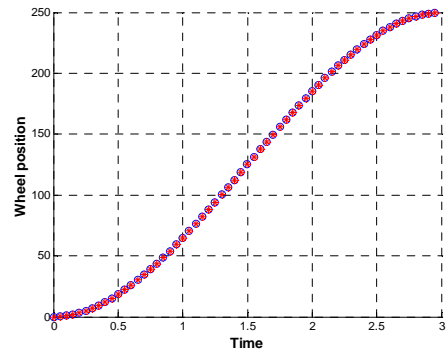


Fig. 6. Simulation result for a straight line trajectory



(a) Velocity profile of the first trailer



(b) Position profile of the first trailer

Fig. 7. Simulation result for a line trajectory

4.3 Simulation for a curved line trajectory

The second trajectory is a curved line with its total arc length of 3m. This arc trajectory is realized by combining a translational forward velocity of 1 m/s with a angular velocity of 0.1rad/s. Again, for simplicity, all three trailers are also initially aligned on the straight line. Fig. 8 represents the planar view of the simulation results. It is observed that the mobile robot follows along the curved line successively. In Fig. 9, it can be noted that magnitudes of velocity and position of the left wheel is greater then those of velocity and position of the right wheel because the trajectory is curved to the right side. And the simulated results for the other trailer are similar to this result as can be seen in Fig. 9.

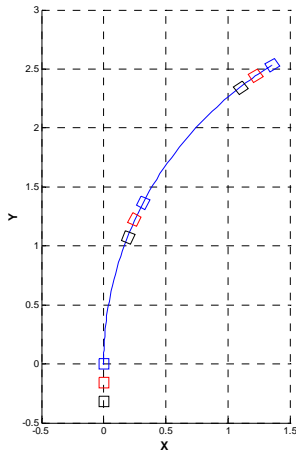
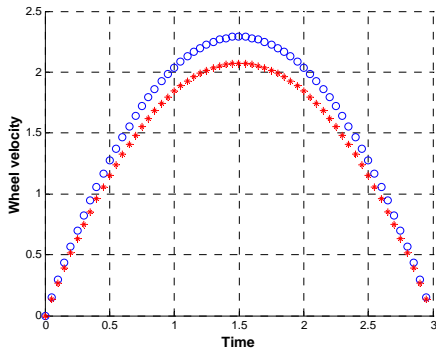
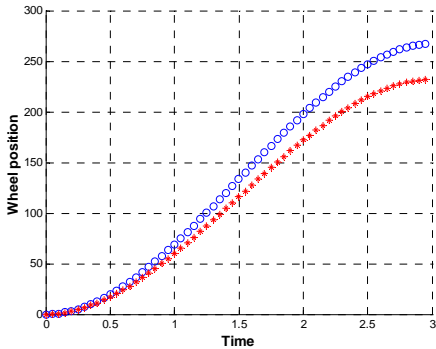


Fig. 8. Simulation result for a curved line trajectory



(a) Velocity profile of the first trailer



(b) Position profile of the first trailer

Fig. 9. Simulation result for a curved line trajectory

4.4 Simulation for a circular trajectory

The third trajectory forms a circle by giving a constant forward velocity - 2m/s and a constant angular velocity 0.2rad/s. The trailers are initially on the straight line and then gradually enter the circle whose radius is given 1m.

Fig. 10 represents the planar view of the simulation result. It can be seen that the mobile robot follows along the circular line successfully.

Note, however, that since the trailers are initially aligned on the straight line as shown in Fig. 10, the first trailer is right on the circular track from the start, while the second and third trailers, which are not on the track, have to enter the circular track with a little swinging. Thus it can be seen from the simulation results that the steering angles of the trailer robot are successively converged to constant values in a short time.

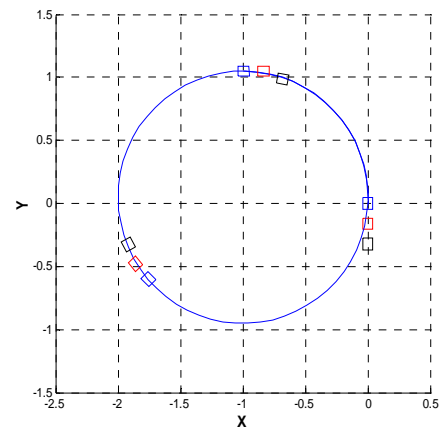


Fig. 10. Simulation result for a circular trajectory

4.5 Simulation for the steering angles

Fig. 11 represents the simulation result of ψ_1 and ψ_2 , which are obtained from Eq. (46). The upper line printed as a series of “*” represents ψ_2 and the lower line as a series of “o” represents ψ_1 .

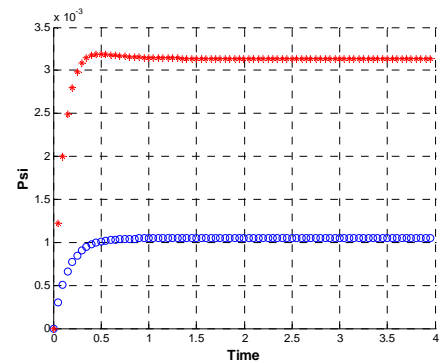


Fig. 11. Simulation result of the steering angles ψ_1 and ψ_2

5. CONCLUSION

In this paper, we focused on the kinematic modeling of chained form mobile robots. Firstly, a closed form kinematic model of chained form mobile robots is derived. Then the effectiveness of this modeling method is confirmed through

various types of trajectory-following simulations for a mobile system consisting of three trailers. We firmly believe that this closed form kinematic model is beneficial to the geometric analysis and design of this kind of chained form mobile systems. Our future work would be 1) to derive a closed form dynamic model of the chained form mobile robot and 2) to investigate the design issue of the chained form mobile robots, based on the closed form kinematic and dynamic models.

REFERENCES

- [1] B.-J. Yi, D.H. Kim, W.K. Kim, and B.-J. You, "Kinematic Modeling of Mobile Robots by Transfer Method of Augmented Generalized Coordinates," Proceedings of the 2001 IEEE International Conference on Robotics and Automation, pp. 2413-2418, May 21-26, 2001.
- [2] J.P. Laumond, "Controllability of a multi-body mobile robot," IEEE Transactions on Robotics and Automation, Vol. 9, No. 6, pp. 755-763, 1993.
- [3] R.M. Murray and S.S. Sastry, "Nonholonomic motion planning : Steering using sinusoids," IEEE Transactions on Automatic Control, Vol. 38, No. 5, pp. 700-716, 1993.
- [4] J.Y. Lee, W.J. Chung, M.S. Kim, C.W. Lee, and J.B. Song, "A passive multiple trailer system for indoor service robots," Proc. Of 2001 IROS, pp. 827-832, 2001.
- [5] D.M. Tilbury, R.M. Murray, and S.S. Sastry, "Trajectory generation for n-trailer problem using Goursat normal form," Proceedings of the IEEE Control and Decision conference, pp. 971-977, 1993.